Electrode-dependent electrical properties of metal/Nb-doped $SrTiO_3$ junctions

C. Park, Y. Seo, J. Jung, and D.-W. Kim'

Citation: Journal of Applied Physics **103**, 054106 (2008); doi: 10.1063/1.2872707
View online: http://dx.doi.org/10.1063/1.2872707
View Table of Contents: http://aip.scitation.org/toc/jap/103/5
Published by the American Institute of Physics

Electrode-dependent electrical properties of metal/Nb-doped $SrTiO_3$ junctions

C. Park,[1] Y. Seo,[1] J. Jung,[1] and D.-W. Kim[2,a)]
[1]*Department of Applied Physics, Hanyang University, Ansan, Kyunggi-do 426-791, Republic of Korea*
[2]*Division of Nano Sciences and Department of Physics, Ewha Womans University, Seoul 120–780, Republic of Korea*

(Received 22 October 2007; accepted 15 December 2007; published online 12 March 2008)

In this study, we discuss the electrical properties of junctions consisting of metal electrodes and Nb-doped $SrTiO_3$(001) single crystals. The junctions formed with large work function metals (Ni, Au, Pd, and Pt) resulted in rectifying transport. A hysteretic feature was observed in the current (I)-voltage (V) and capacitance (C)-V characteristics of these junctions upon polarity reversal. The ideal Schottky–Mott rule could not explain the barrier height obtained from the I-V data, indicating the existence of interface states. Analyses of the C-V data revealed that a low dielectric constant layer existed at the interface. The interface states and layers affected the transport and the related resistance switching characteristics of the junctions. © *2008 American Institute of Physics*. [DOI: 10.1063/1.2872707]

I. INTRODUCTION

Electric-field- and/or current-induced resistance switching phenomena in metal oxides, referred to as colossal electroresistance (CER) effects, have attracted considerable research interest due to their potential use in nonvolatile memory device applications.[1–12] The root cause of CER has not been identified. Several models have been proposed to explain the phenomena, including the formation/rupture of conducting filaments,[1,2] charge trapping in trap states,[3] a Mott transition induced by carrier doping,[4] an electrochemical migration of oxygen vacancies,[6] a Schottky-like barrier alteration,[8] and so on. Studies of thin films and single crystals clearly show that the dominant mechanism of CER depends not only on the material but also on its crystalline form.[5–8] Bulk defects in thin films, which are practically unavoidable in thin-film formation, have been believed to play key roles in the CER behaviors.[1–3,5] Single crystals, on the other hand, have little crystalline disorder and compositional variation. Thus, the resistance switching of metal/Nb-doped $SrTiO_3$ (Nb:STO) single-crystal junctions has been attributed to an interface effect.[6–8] The junction characteristics, such as barrier height and interface states, should be closely related to the CER phenomena of metal/Nb:STO junctions. Comparative studies of electrode materials have not been explicitly attempted.[9–12] Such studies will help elucidate the interface-related CER mechanism.

In this paper, we describe the electrical properties of metal/Nb:STO single-crystal junctions. The junctions formed with large work function metals showed rectifying transport behavior, and their current (I)-voltage (V) and capacitance (C)-V characteristics showed a hysteretic feature. Analyses of the I-V and C-V data suggested that interface states and a low dielectric constant layer existed. The roles of the interface states and layers in the transport and the CER characteristics of the junctions are discussed.

a)Electronic mail: dwkim322@yahoo.com.

II. EXPERIMENT

This study was conducted using Nb:STO(001) single crystals with a doping ratio of 0.1 wt % (CrysTec, GmbH, Germany). The samples were annealed at 1000 °C in flowing O_2 for 1 h to obtain a flat surface. Metal electrodes were deposited onto the Nb:STO surface using an e-beam evaporator (base pressure: $<10^{-7}$ Torr) with a shadow mask (electrode area of 100×100 μm^2). The Ti and Ni electrodes (thickness: 10 nm) were capped with Au layers (thickness: 30 nm) to prevent oxidation. The Pt and Pd layers (thickness: 10 nm) were also coated with Au layers (thickness: 30 nm) to ensure comparable contact to the probe tips. Films of Au (30 nm) and Ti (10 nm) were evaporated onto the back sides of the samples to obtain the Ohmic contact. I-V characteristics were measured using a Keithley 2400 sourcemeter between ±1 V. C-V characteristics were investigated using an Agilent 4294A impedance analyzer from -1 to $+1$ V with a test signal of 50 mV. No obvious frequency dependence was observed between 10 kHz and 1 MHz in the C-V characteristics. Figure 1(a) illustrates the junction structure and the measurement configuration.

III. RESULTS AND DISCUSSIONS

A. *I-V* characteristics

Figure 1(b) shows typical I-V curves obtained from the junction of the Nb:STO with various metal electrodes. We defined the current direction from the top electrode as positive and the opposite one as negative. We measured the current values while sweeping the voltage from -1 to $+1$ V. The junctions formed with high work function metals (Ni, Pt, Pd, and Au) had much lower current levels than the Ti/Nb:STO junction. This indicates that the top electrode/Nb:STO contact dominates the transport properties of the junctions. Since Nb:STO is a n-type semiconductor with a band gap of 3.3 eV,[13] the barrier heights of low work function (ϕ_M) metals, such as Ti (ϕ_M=4.33 eV), are smaller and

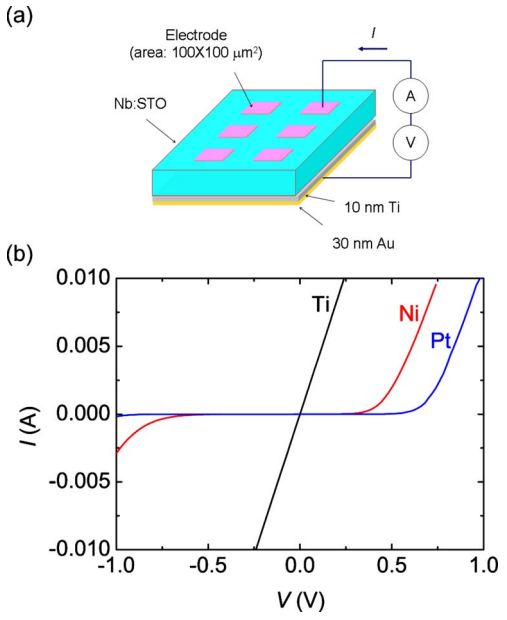

FIG. 1. (Color online) (a) Schematic diagram of the metal/Nb:STO junction structure and the configuration for the *I-V* measurements, where the arrow indicates the positive current direction. (b) Typical *I-V* curves of the metal/0.1 wt % Nb:STO junctions with three kinds of electrodes (Ti, Ni, and Pt).

can allow Ohmic behavior. On the other hand, large work function metals such as Ni (ϕ_M=5.15 eV), Au (ϕ_M =5.1 eV), Pd (ϕ_M=5.12 eV), and Pt (ϕ_M=5.65 eV) induce large barriers, causing rectifying behavior.

The rectifying junctions also exhibited hysteretic behavior, as shown in Fig. 2. The switching from a high-resistance state (HRS) to a low-resistance state (LRS) occurs during the positive (forward) bias scan to 1.0 V, and the reverse switching occurs during the negative (reverse) bias scan to −1.0 V. Thus, the resistance switching requires a bias polarity reversal. The *I-V* curves are very reproducible for 50 voltage scans. This indicates that our metal/Nb:STO junctions do not undergo any irreversible chemical or structural changes during repetitive measurements.[9–11]

The current in the positive bias region increases exponentially, much like a conventional Schottky diode. In addition, a relatively large current is seen in the reverse bias region. This observation is consistent with the results of previous studies of Nb:STO-based junctions.[7,14–19] We can assume, therefore, that the transport properties of our metal/

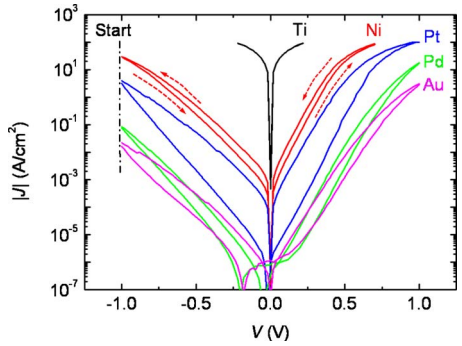

FIG. 2. (Color online) *J-V* curves of the M/Nb:STO junctions with various electrodes.

TABLE I. n and ϕ_B values of the LRS and HRS.

	Barrier height ϕ_B (V)		Ideality factor n	
Electrode	HRS	LRS	HRS	LRS
Au	0.88	0.84	2.16	2.00
Ni	0.63	0.61	1.57	1.57
Pd	0.87	0.82	1.90	1.90
Pt	0.77	0.67	1.60	1.63

Nb:STO junctions can be explained using a Schottky diode model. The forward current density J_F can be expressed as

$$J_F = J_S \exp(-qV/nk_BT), \tag{1}$$

$$J_S = A^*T^2 \exp(-q\phi_B/k_BT), \tag{2}$$

where A^* is the Richardson constant, n is the ideality factor, k_B is the Boltzmann constant, q is the electron charge, and ϕ_B is the Schottky barrier height.[21] The junction parameters n and ϕ_B can be estimated from the slope and intercept of the current axis in Fig. 2, respectively. The estimated values for the LRS and the HRS are shown in Table I.

The simple Schottky—Mott relationship $\phi_B=\phi_M-\chi_S$ (where ϕ_B is the barrier height and χ_S is the electron affinity of the semiconductor) predicts ideal barrier heights for the junctions: ϕ_B (Ni) ~ ϕ_B(Au) ~ 1.2 eV and ϕ_B (Pt) ~ 1.7 eV.[13,21] These values are much larger than those shown in Table I. The discrepancy indicates that the simple electron affinity rule is inappropriate for our metal/Nb:STO junctions. Interface states and interfacial reactions seem to affect the barrier height of our junction.[20]

Also, it can be noted that the ideality factors (n) of our junctions deviate greatly from unity. There are several factors that contribute to an increase of n: tunneling contribution to the transport, conduction through interface states, and the voltage dependence of the barrier height.[7,15–17] Since the relative permittivity of STO (over 300 at room temperature) is much larger than that of conventional semiconductors, the depletion width is much larger than those of Si or GaAs junctions. This means that direct tunneling currents through the barrier are low.[15] The existence of the interface states and the insulating interfacial layers may explain the increase of n.

B. *C-V* characteristics

Figure 3 shows the *C-V* characteristics of the metal/Nb:STO junctions measured at 1 MHz. The hysteresis of the capacitance assures a barrier height alteration, which can be caused by charge trapping in interface states and/or oxygen vacancy migration.[7,8] There are two possible origins of the interface states between the metal and the semiconductor. One is induced by extrinsic effects, such as carbon contamination or a reaction layer. The other is caused by intrinsic effects, including atomic rearrangement of the oxide and the reduction of an interdipole interaction in a dipole at the interface.[15–17] In our experiments, all of the electrodes were prepared using an identical evaporation technique. Hence,

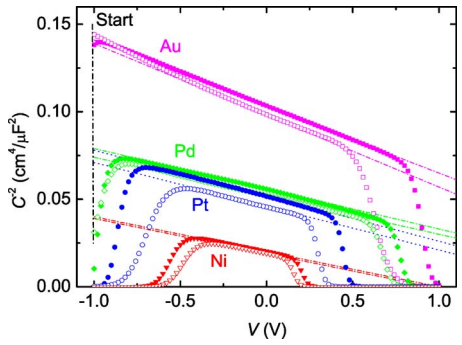

FIG. 3. (Color online) $1/C^2$-V curves of the M/Nb:STO junctions with various electrodes.

the contaminant effects cannot explain all of the experimental results, especially the electrode material dependence.

Sawa *et al.* reported that $SrRuO_3$/Nb:STO junctions showed rectifying I-V characteristics similar to our junctions.[7] There are some distinctions between the epitaxial heterojunction and our junctions. First, the $SrRuO_3$/Nb:STO junctions did not exhibit hysteresis in the C-V characteristics. Second, the log I-V curves were well above the straight lines predicted from a standard Schottky diode model in the low bias voltage region (<1 V). The excess current was more prominent for the junctions with a higher Nb-doping ratio. Based on these results, the authors proposed that tunneling through the interface trapping states contributed to the junctions' conduction. The difference between the epitaxial $SrRuO_3$ thin film and the metal electrodes suggests that the interface transport is very sensitive to the electrode material and sample preparation procedures.

Figure 4 shows that the $1/C^2$-V curves for our junctions are almost linear under the low voltage reverse bias region. Large current under the large bias region hinders reliable C-V measurements. Conventional Schottky junctions at the reverse bias region have the following relationship:

$$1/C^2 = (V_{\mathrm{bi}} - V - k_B T/q)/q\varepsilon_S N_D, \tag{3}$$

where V_{bi} is the built-in potential, and ε_S and N_D are the dielectric constant and the donor concentration of Nb:STO, respectively. V_{bi} and $\varepsilon_S N_D$ can be extracted from the intersection and slope of the straight lines fitted to the experimental data, as shown in Fig. 4. Such analyses reveal several extraordinary facts. First, the slope of the $1/C^2$-V curve (proportional to $1/\varepsilon_S N_D$) is different for each electrode. All of the electrodes were deposited on the same Nb:STO sample in our study, so $\varepsilon_S N_D$ should be the same. Second, the extrapolated C-V curves yield very large V_{bi}: 2.65, 2.55, and 2.06 eV for Au, Pd, and Pt, respectively. These values are much larger than ϕ_B and also larger than half of the STO band gap (3.3 eV).[13] Yoshida *et al.* explained the lower capacitance and higher built-in potentials of the Au/Nb:STO junctions by assuming a low dielectric constant interfacial layer.[15] The total junction capacitance C can be written in the following form:

$$1/C = 1/C_i + 1/C_d, \tag{4}$$

where C_i and C_d are the capacitances of the interfacial layer and the depletion layer, respectively. The total applied voltage V also can be written as

$$V = V_i + V_d, \tag{5}$$

where V_i and V_d are the voltages applied to the interfacial layer and the depletion layer, respectively.

As noted in Fig. 4, the $1/C^2$-V curves deviate slightly from a straight line. This slight nonlinear behavior may be caused by the electric field dependent permittivity ε_S of STO: $\varepsilon_S = b/(a+E^2)^{1/2}$ ($a = 1.64\times10^{15}$ V^2/m^2 and $b = 1.42\times10^{10}$ V^2/m^2).[15–18] Hikita *et al.* derived the junction capacitance as

$$1/C_d^2 = 2\sqrt{a}(V_{\mathrm{bi}} - V_d - k_B T/q)(bq\varepsilon_0 N_D) + (V_{\mathrm{bi}} - V_d - k_B T/q)^2/(b\varepsilon_0)^2, \tag{6}$$

where ε_0 is the vacuum permittivity and N_D is the doping concentration (2.3×10^{19} cm^{-3}).[18] The C-V data can be analyzed using Eqs. (4)–(6), and properly chosen C_i and V_{bi} values can reproduce the experimental data shown in Fig. 4. The estimated V_{bi} values (0.8–1.2 eV) are close to the ϕ_B values. The C_i value for our Au/Nb:STO junction (6.2×10^{-6} F/cm^2) is also comparable to the value reported by Yoshida *et al.* (9.5×10^{-6} F/cm^2).[15] In addition, the $\Delta\phi_B = (\phi_{B,\mathrm{HRS}} - \phi_{B,\mathrm{LRS}})$ and $\Delta V_{\mathrm{bi}} = (V_{\mathrm{bi,HRS}} - V_{\mathrm{bi,LRS}})$ values are similar. All of these results suggest that the model used in our analyses is appropriate.

Figure 5(a) shows n and C_i for the junctions: the junctions with larger C_i values have smaller n values. This manifests the presence of the interface layer of our junctions. Since part of the bias voltage is dropped across the insulating interface layer, the barrier height should depend on the bias voltage. The interface layer thickness δ_i is related to C_i according to the relation $C_i = \varepsilon_i/\delta_i$. Thus, an increase of δ_i (i.e., decrease of C_i) will raise n.[16]

Figure 5(b) shows the extracted ϕ_B and V_{bi} for the HRS of our junctions. V_{bi} is larger than ϕ_B by about 0.1 (0.4) eV for the Ni, Au, and Pd (Pt) electrodes. In an ideal junction, the difference $V_{\mathrm{bi}} - \phi_B$ corresponds to the depth of the Fermi level below the conduction band minimum. In Nb:STO, this difference is about 0.1 eV,[18] which is comparable to the results for the Ni, Au, and Pd electrodes. In real junctions, any nonhomogeneity at the interface can alter the local barrier height, and defects may act as intermediate states for trap-assisted tunnel currents.[20] Either of these anomalies can

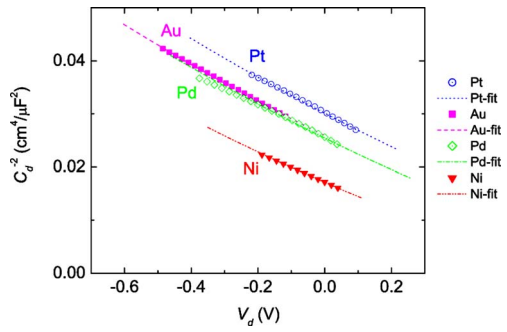

FIG. 4. (Color online) $1/C_d^2$-V_d curves of the M/Nb:STO junctions with various electrodes. The symbols and dotted lines indicate the experimental data and fitting results, respectively.

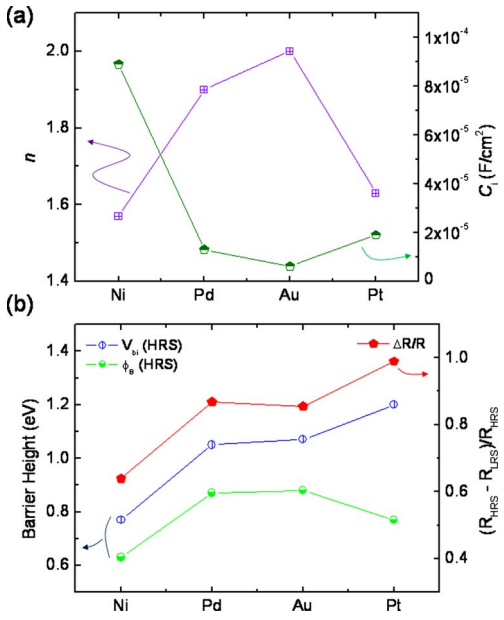

FIG. 5. (Color online) (a) The junction parameters (n and C_i) and (b) barrier height (ϕ_B and V_{bi}) for the HRS and the resistance switching ratio of the M/Nb:STO junctions with various electrodes.

lower ϕ_B in the I-V characteristics. C-V measurements are less prone to such local fluctuation since the barrier height with the largest contact area dominates the C-V behavior. Therefore, the large $V_{bi}-\phi_B$ value for the Pt junction indicates that the barrier height fluctuation and/or trap-mediated conduction can be significant.

Figure 5(b) clearly shows that the resistance switching ratio, $(R_{HRS}-R_{LRS})/R_{HRS}$, has a tendency similar to that of V_{bi}. (No clear relationship can be found between the interface capacitance and the resistance switching ratio.) To explain such trends, a possible mechanism can be proposed as follows. First, a large barrier height will increase the maximum electric field (E_{max}) in the depletion region, $E_{max}=[2qN_D(V_{bi}-V-k_BT/q)/\varepsilon_S]^{1/2}$.[20] The electric field can promote the charge trapping/detrapping in the interface states[9] and/or oxygen vacancy migration.[10] Second, interfacial reactions such as the oxidation of metals and metal encapsulation can be enhanced under a large electric field at the interface.[21] Either of these mechanisms can alter the barrier height and the junction resistance.

Interfacial reaction effects on the transport are evident from the Ni/Nb:STO junction results. It possesses a smaller barrier height compared with those of the noble metal (Pd, Au, and Pt)/Nb:STO junctions. The Ni/Nb:STO junction has the smallest V_{bi} and ϕ_B, and the largest C_i. This supports the idea that the reaction (oxidation) occurs at the Ni/Nb:STO interface, resulting in the lowering of the barrier height and the reduction of the interface layer thickness. Moreover, the hysteretic I-V behavior disappeared after annealing the Ni/Nb:STO junctions at 300 °C for 30 min. (All of the other junctions with Pd, Au, and Pt still exhibited the hysteresis after the same heat treatment.) These results suggest that interfacial oxygen vacancy concentration may be involved in the interface state formation and the related resistance switching behaviors of our junctions.

IV. CONCLUSIONS

The rectifying metal/Nb:STO junctions formed with high work function metal electrodes (Ni, Pd, Au, and Pt) exhibited hysteretic I-V and C-V characteristics. Junction parameters, such as barrier heights, built-in potentials, ideality factors, and interface layer capacitance, were extracted from analyses of the electrical properties. The barrier height, predicted from the Schottky–Mott rule, was largely different from the estimated results. The presence of the interface states and insulating interface layers was also noticed. The relationship between the junction parameters and the resistance switching ratio was examined: the junction with larger built-in potential showed larger resistance switching ratio. The resistance switching ratio did not show explicit dependence on the other junction parameters. The interface states, presumably related to oxygen vacancies, seemed to play crucial roles in the resistance switching behaviors at the metal/Nb:STO interface.

ACKNOWLEDGMENTS

This work was supported by the Korea Research Foundation Grant funded by the Korean Government (MOEHRD) (KRF-2007-331-C00083).

[1] S. Seo, M. J. Lee, D. H. Seo, E. J. Jeoung, D.-S. Suh, Y. S. Joung, I. K. Yoo, I. R. Hwang, S. H. Kim, I. S. Byun, J.-S. Kim, J. S. Choi, and B. H. Park, Appl. Phys. Lett. **85**, 5655 (2004).
[2] K. M. Kim, B. J. Choi, Y. C. Shin, S. Choi, and C. S. Hwang, Appl. Phys. Lett. **91**, 012907 (2007).
[3] A. Chen, S. Haddad, Y. C. Wu, Z. Lan, T. N. Gang, and S. Kaza, Appl. Phys. Lett. **91**, 123517 (2007).
[4] M. J. Rozenberg, I. H. Inoue, and M. J. Sánchez, Phys. Rev. Lett. **92**, 178302 (2004).
[5] D. Choi, D. Lee, H. Sim, M. Chang, and H. Hwang, Appl. Phys. Lett. **88**, 082904 (2006).
[6] K. Szot, W. Speier, G. Bihlmayer, and R. Waser, Nat. Mater. **5**, 312 (2006).
[7] T. Fujii, M. Kawasaki, A. Sawa, Y. Kawazoe, H. Akoh, and Y. Tokura, Phys. Rev. B **75**, 165101 (2007).
[8] S. H. Jeon, B. H. Park, J. Lee, B. Lee, and S. Han, Appl. Phys. Lett. **89**, 042904 (2006).
[9] A. Sawa, T. Fujii, M. Kawasaki, and Y. Tokura, Appl. Phys. Lett. **85**, 4073 (2004).
[10] K. Tsubouchi, I. Ohkubo, H. Kumigashira, M. Oshima, Y. Matsumoto, K. Itaka, T. Ohnishi, M. Lippmaa, and H. Koinuma, Adv. Mater. (Weinheim, Ger.) **19**, 1711 (2007).
[11] H.-S. Lee, J. A. Bain, S. Choi, and P. A. Salvador, Appl. Phys. Lett. **90**, 202107 (2007).
[12] Y. Tokunaga, Y. Kaneko, J. P. He, T. Arima, A. Sawa, T. Fujii, M. Kawasaki, and Y. Tokura, Appl. Phys. Lett. **88**, 223507 (2006).
[13] J. Robertson, J. Vac. Sci. Technol. B **18**, 1785 (2000).
[14] W. Ramadan, S. B. Ogale, S. Dhar, L. F. Fu, S. R. Shinde, D. C. Kundaliya, M. S. R. Rao, N. D. Browning, and T. Venkatesan, Phys. Rev. B **72**, 205333 (2005).
[15] A. Yoshida, H. Tamura, K. Gotoh, H. Takauchi, and S. Hasuo, J. Appl. Phys. **70**, 4976 (1991).
[16] S. Suzuki, T. Yamamoto, H. Suzuki, K. Kawaguchi, K. Takahashi, and Y. Yoshisato, J. Appl. Phys. **81**, 6830 (1997).
[17] T. Shimizu and H. Okushi, J. Appl. Phys. **85**, 7244 (1999).
[18] Y. Hikita, Y. Kozuka, T. Susaki, H. Takagi, and H. Y. Hwang, Appl. Phys. Lett. **90**, 143507 (2007).
[19] R. A. van der Berg, P. W. Blom, J. F. M. Cillessen, and R. M. Wolf, Appl. Phys. Lett. **66**, 697 (1995).
[20] S. M. Sze and K. K. Ng, *Physics of Semiconductor Devices*, 3rd ed. (Wiley, Hoboken, 2007).
[21] Q. Fu and T. Wagner, J. Phys. Chem. B **109**, 11697 (2005).